

This article was downloaded by: [University of California, San Diego]

On: 07 August 2012, At: 12:04

Publisher: Taylor & Francis

Informa Ltd Registered in England and Wales Registered Number: 1072954 Registered office: Mortimer House, 37-41 Mortimer Street, London W1T 3JH, UK



Molecular Crystals and Liquid Crystals

Publication details, including instructions for authors and subscription information:

<http://www.tandfonline.com/loi/gmcl20>

Selenization of Cu-In-Ga Metal Precursor Using DESe(Diethyl Selenide)

Jinu Seo ^a, Sang-Hwan Lee ^a, Soon-Yong Park ^a, Eun-Woo Lee ^a, Woo-Nam Kim ^a, Jung-Ik Ko ^b, Jin-Yeong Do ^b, Wan-Woo Park ^b & Chan-Wook Jeon ^a

^a Department of Chemical Engineering, Yeungnam University, Gyeongsan, 712-749, Korea

^b AVACO Inc., Daegu, Korea

Version of record first published: 18 Oct 2011

To cite this article: Jinu Seo, Sang-Hwan Lee, Soon-Yong Park, Eun-Woo Lee, Woo-Nam Kim, Jung-Ik Ko, Jin-Yeong Do, Wan-Woo Park & Chan-Wook Jeon (2011): Selenization of Cu-In-Ga Metal Precursor Using DESe(Diethyl Selenide), *Molecular Crystals and Liquid Crystals*, 551:1, 249-256

To link to this article: <http://dx.doi.org/10.1080/15421406.2011.601169>

PLEASE SCROLL DOWN FOR ARTICLE

Full terms and conditions of use: <http://www.tandfonline.com/page/terms-and-conditions>

This article may be used for research, teaching, and private study purposes. Any substantial or systematic reproduction, redistribution, reselling, loan, sub-licensing, systematic supply, or distribution in any form to anyone is expressly forbidden.

The publisher does not give any warranty express or implied or make any representation that the contents will be complete or accurate or up to date. The accuracy of any instructions, formulae, and drug doses should be independently verified with primary sources. The publisher shall not be liable for any loss, actions, claims, proceedings, demand, or costs or damages whatsoever or howsoever caused arising directly or indirectly in connection with or arising out of the use of this material.

Selenization of Cu-In-Ga Metal Precursor Using DESe(Diethyl Selenide)

JINU SEO,¹ SANG-HWAN LEE,¹ SOON-YONG PARK,¹
EUN-WOO LEE,¹ WOO-NAM KIM,¹ JUNG-IK KO,²
JIN-YEONG DO,² WAN-WOO PARK,²
AND CHAN-WOOK JEON^{1,*}

¹Department of Chemical Engineering, Yeungnam University, Gyeongsan
712-749, Korea

²AVACO Inc., Daegu, Korea

In this study, Cu(In,Ga)Se₂ thin films were prepared using a Cu-In-Ga metallic precursor and diethylselenide (DESe) vapor. The Cu/(In+Ga) ratio of the precursor was adjusted by modulating the power impressed on the CuGa target. The Cu/(In+Ga) ratio was varied from 0.45 to 1.02, and the prepared precursors were selenized in a 500°C quartz furnace using DESe. The results showed that the preferred crystal phase and the uniformity of the thin film differed according to the composition of the precursor. After selenization, changes in grain size stemming from Cu composition were observed, and the occurrence of a binary phase was verified through KCN etching. Shifts in the Cu₁₁(InGa)₉ peak and the separation of CIS and CGS peaks relative to increased Ga content were also observed.

Keywords: Cu(InGa)Se₂; thin film solar cell; chalcopyrite; precursor; sputter CIGS; diethylselenide

Introduction

Cu(In,Ga)Se₂, as a thin film photovoltaic absorption layer, is generally made using the two-step process of Cu-In-Ga metal precursor sputtering followed by either selenization or co-evaporation. The two-step process is expected to allow better yield management for a large area module. The selenization process is normally performed using a highly reactive H₂Se gas or safe Se vapor. However, H₂Se gas is highly hazardous and needs a special scrubbing facility, while it is difficult to realize large area uniformity with Se vapor due to its low chemical activity. On the other hand, diethylselenide (DESe) is less hazardous [1,2] and has a lower binding energy than either H₂Se gas or Se vapor. While the binding energy of H-Se and Se = Se is 276 and 332 kJ/mol, respectively, the binding energy of Se-C₂H₅ is significantly lower at 243 kJ/mol, making it the most suitable for use in supplying Se to the precursor. In a previous study on selenization using Se vapor, the current research group experimentally confirmed such problems as the non-uniformity of selenization and a severe deficiency in the amount of incorporated Se, which was 45at% or less (not shown here). Despite the many advantages of DESe, its applicability in the fabrication of CIGS

*Corresponding author. E-mail: cwjeon@ynu.ac.kr

absorption layers has not yet been systematically investigated. Therefore, in this paper, selenization was performed using a precursor and DESe while varying the Cu/(In+Ga) ratio of the precursor, in order to observe the resulting changes.

Experimentals

Precursor Deposition

Metal precursor films used in this study were deposited on 25×25 mm molybdenum-coated soda-lime glass substrates. Deposition was carried out via the magnetron co-sputtering system using 3-inch In and a CuGa (Ga, 24wt%) metal target. For In deposition, DC power was used; for CuGa deposition, RF power was used. To ensure the uniformity of the thin film, the stage was spun at 10 rpm and no additional heat was applied. For plasma gas, Ar gas (99.999% impurity) was used, with the working pressure maintained at 1mtorr (0.13Pa).

With the DC power fixed, the RF power impressed on the CuGa target was varied to adjust the Cu ratio of the precursor from 0.45 to 1.02. Then, sputtering time was adjusted to achieve a thickness of 500–600 nm.

Composition and thickness analysis was performed using Inductively Coupled Plasma (ICP) and Alpha-Step. X-ray diffraction (XRD) was used to determine the crystallography of the precursor, while its morphology was observed using a scanning electron microscope (SEM).

Selenization

Selenization was carried out in a resistive heated quartz furnace. Selenization temperature was 500°C, and the ramp-up speed from room temperature to the target temperature was 22.7°C/min [3]. Once the temperature reached 500°C, reaction was induced for 10 minutes, then cooling was carried out over 20 minutes. The N₂ (99.999% impurity) used as the carrier gas for DESe was added simultaneously with ramp up at a rate of 1L/min, with additional N₂ (99.999% impurity) injected into the chamber to maintain atmospheric pressure [4]. Also, to control DESe vapor pressure at a constant level, the DESe bottle was kept at 10°C using a water bath.

Composition was ascertained using Inductively Coupled Plasma (ICP). X-ray diffraction (XRD) was used to determine the crystallography of the precursor, while its morphology was observed using a scanning electron microscope (SEM).

Results and Discussion

Precursor

The composition of the precursor films determined by ICP is given in Table 1-(a). As the Cu/(In+Ga) ratio increases, the Ga/(In+Ga) ratio also increases linearly, an effect that can be attributed to the use of a CuGa alloy target.

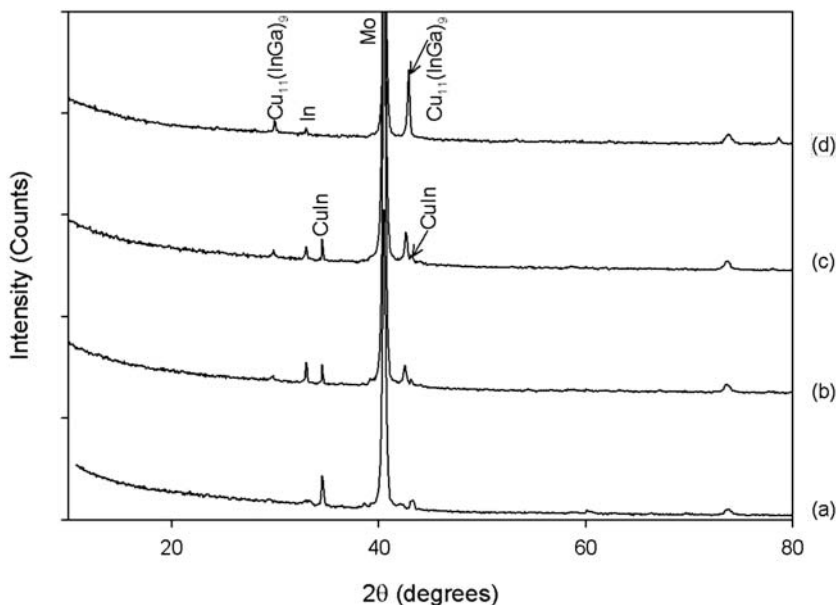
From the XRD peaks of the precursor films shown in Figure 1, it can be seen that an increase in the Cu/(In+Ga) ratio causes the Cu₁₁(InGa)₉ peak to manifest more strongly while causing the CuIn peak to disappear. This appears to be because the preferred crystal phase of the precursor changes according to the Cu ratio, with the configuration starting as CuIn in the Cu-poor state, then shifting to Cu₁₁(InGa)₉ as the Cu ratio grows higher.

Table 1. Inductively Coupled Plasma (ICP) data of (a) CuInGa precursor, (b) CIGS after selenization.

	Cu/(Ga+In)	Ga/(In+Ga)	Mol Fraction (In+Ga)=1			
			Cu	In	Ga	Se
Precursor (a)	0.45	0.15	0.45	0.85	0.15	–
	0.73	0.23	0.73	0.77	0.23	–
	0.89	0.27	0.89	0.73	0.27	–
	1.02	0.29	1.02	0.71	0.29	–
After Selenization (b)	0.45	0.17	0.45	0.83	0.17	1.63
	0.69	0.24	0.69	0.76	0.24	2.00
	0.81	0.25	0.81	0.75	0.25	2.09
	1.34	0.38	1.34	0.62	0.38	2.35

A particularly interesting observation regarding the XRD peaks of the CuInGa precursor shown in Figure 2 is that the main peak of the $\text{Cu}_{11}(\text{InGa})_9$ (312) shifts from 42.274° to 42.833° as the Cu ratio increases. This is due to the fact that the Ga content changed along with the Cu ratio, as can be seen in Table 1-(a). Hence, as Ga content increases, the amount of In in $\text{Cu}_{11}(\text{InGa})_9$ that is substituted by Ga, whose atomic radius is comparatively smaller, also increases, which causes the peak to shift to the right. The peak shift calculated according to the Vegard's law equation is shown in Figure 3.

Figure 4 shows the SEM images of the precursors with varying Cu/(In+Ga) ratios. As can be seen, the surface becomes more uniform as the Cu/(In+Ga) ratio grows higher.

**Figure 1.** XRD patterns of co-sputtered Cu-In-Ga alloy film with different Cu/(In+Ga) ratios ranging; (a) 0.45, (b) 0.73, (c) 0.89, (d) 1.02.

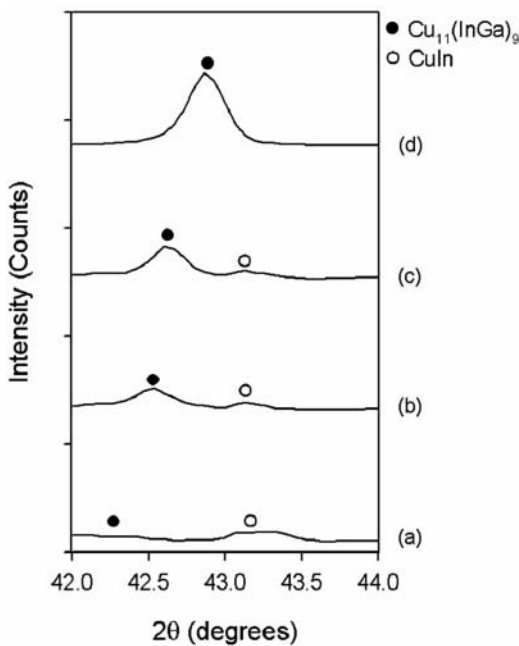


Figure 2. XRD patterns of (312) reflection of $\text{Cu}_{11}(\text{InGa})_9$ and CuIn with different $\text{Cu}/(\text{In}+\text{Ga})$ ratios ranging; (a) 0.45, (b) 0.73, (c) 0.89, (d) 1.02.

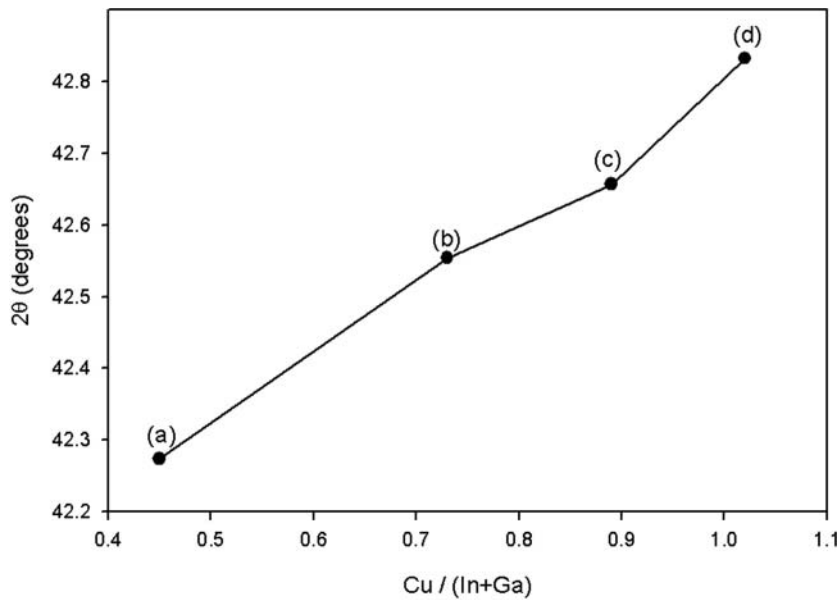


Figure 3. (312) peak shift based on the ratio of $\text{Cu}/(\text{In}+\text{Ga})$ in precursor; (a) 0.45, (b) 0.73, (c) 0.89, (d) 1.02.

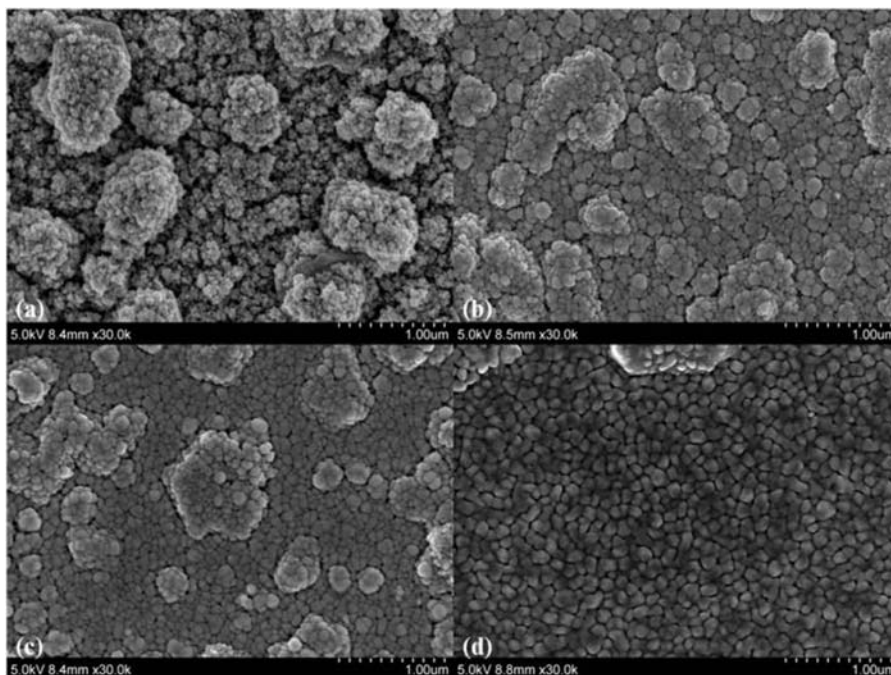


Figure 4. Surface SEM images of Cu-In-Ga precursor with different Cu/(In+Ga) ratios ranging; (a) 0.45, (b) 0.73, (c) 0.89, (d) 1.02.

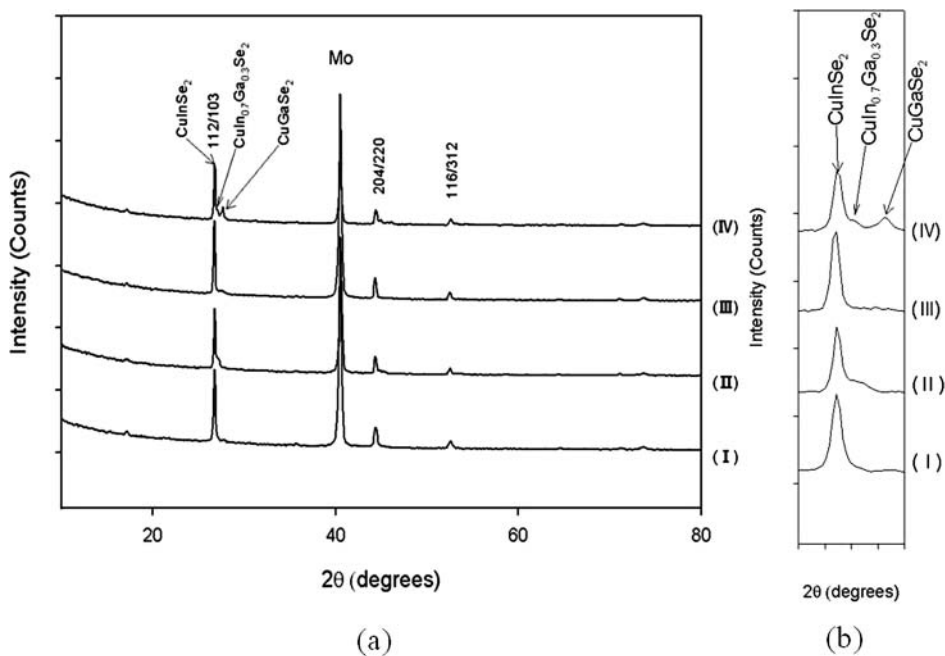


Figure 5. XRD patterns of (a) selenized precursor and (b) enlarged (112) peaks with different Cu/(In+Ga) ratios of (I) 0.45, (II) 0.73, (III) 0.89, (IV) 1.02.

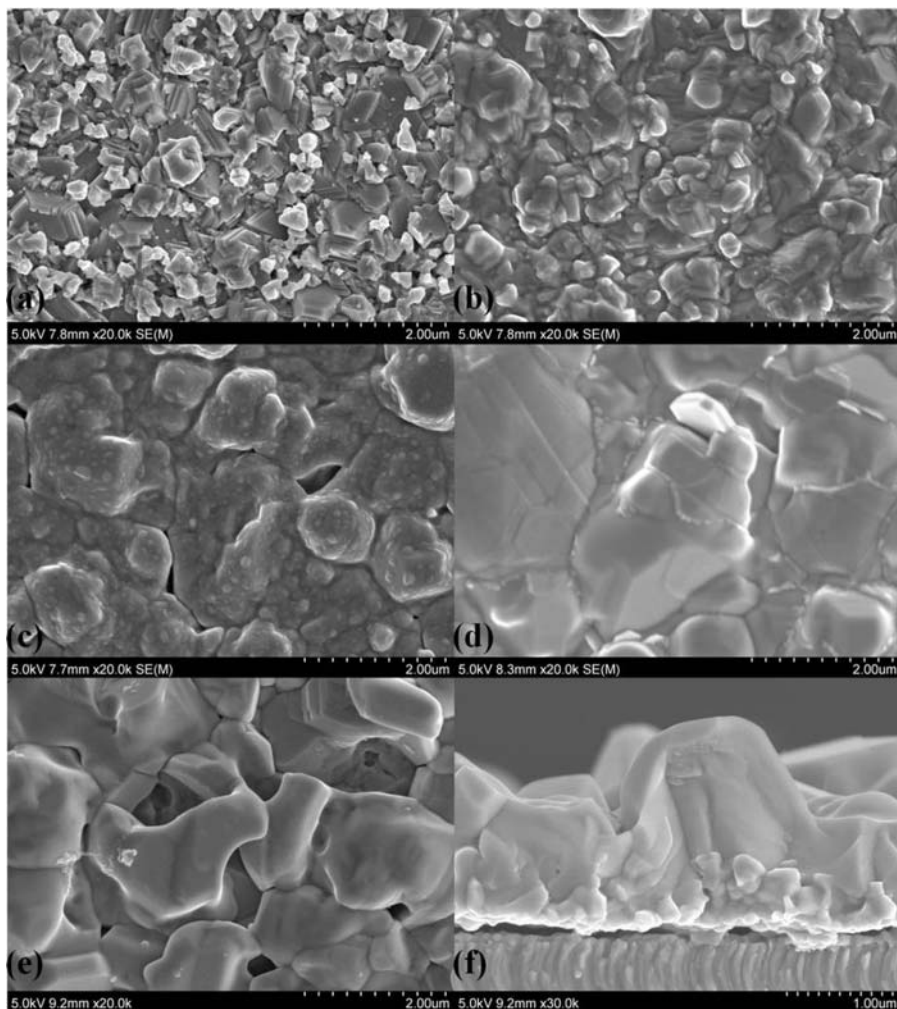


Figure 6. Surface SEM images of selenized precursor with different Cu/(In+Ga) ratios; (a) 0.45, (b) 0.73, (c) 0.89, (d) 1.02. The (e) is CIGS film after KCN etching of (c) precursor, and (f) is cross-sectional image of (d) precursor after KCN etching.

In Cu-poor precursors, In-rich islands form on the surface [5,6], resulting in exacerbated surface roughness.

Selenization

Table 1-(b) shows the ICP data after selenization. It can be seen that the Ga/(In+Ga) ratio has become higher than the ratio of the precursor (Table 1-(a)) as a result of selenization. This Ga/(Ga+In) ratio increase is due to the evaporation of In in volatile InSe form during high-temperature thermal treatment [7].

The post-selenization XRD data is given in Figure 5. It can be seen in Figure 5-(b) that the $\text{CuIn}_{0.7}\text{Ga}_{0.3}\text{Se}_2$ peak and the CuGaSe_2 peak begin to manifest as the Cu ratio changes. As shown in Table 1, the Ga/(In+Ga) ratio grows increasingly higher from (a) to (b). In

our study, an increase in the Ga/(In+Ga) ratio did not cause the main peaks to shift, as reported in [4], but rather caused the CuGaSe₂ peak to emerge. In [4], the CuIn_{0.7}Ga_{0.3}Se₂ peak shifted as a result of Ga substitution, but in the current study the peaks for CuInSe₂ and CuGaSe₂ were seen to exist separately from each other. This can be attributed to the fact that our experiment was based on a 10-minute reaction time, rather than the 90 minutes seen in [4], which did not allow for sufficient time for Ga to be substituted into CuInSe₂. In Figure 5, (IV) has the highest Ga content; in this case, a CuIn_{0.7}Ga_{0.3}Se₂ peak starts to emerge in the form of a shoulder, indicating that CuIn_{0.7}Ga_{0.3}Se₂ formation has begun even with 10 minutes of reaction time. In the cross-sectional SEM image provided in Figure 6-(f), a section that is presumably a CuGaSe₂ layer can be observed close to the Mo layer.

The SEM surface images provided in Figure 6-(a) through (d) show that grain size increases as the Cu/(In+Ga) ratio grows higher. Large grains can have a lowering effect on series resistance. In the most Cu-rich sample, hexagonal crystals that are different from CuInSe₂ can be seen embedded in between the grains. These crystals appear to be CuSe, formed through the reaction of excess Cu and Se in the Cu-rich composition [8]. Figure 5-(e) shows the surface of the selenized precursor with Cu/(Ga+In) = 1.02 composition after KCN etching, as seen through an SEM. The image shows that the crystals presumed to be CuSe have disappeared, leaving large pores in their wake. Among the conductive binary phases that can be removed through KCN etching, such as CuSe, Cu₂Se, and Cu_{2-x}Se, CuSe is the only one that has the large, hexagonal planar shape observable in Figure 6-(e). Therefore, it can be concluded that the crystals seen between the grains in the Cu-rich precursor shown in Figure 6-(d) are in fact CuSe.

Conclusions

In this study, we observed the co-sputtering of CuInGa film while varying the power impressed on the CuGa target, and analyzed the results of selenization in a quartz furnace using the less-hazardous DESe.

In summary, the precursor film takes on a smoother surface and inclines increasingly toward the Cu₁₁(InGa)₉ phase as it becomes richer in Cu. It also produces larger CIGS grains, thus helping to lower the series resistance of the resulting device. However, if the Cu content becomes excessively high, such second phases as CuSe can occur in substantial quantities after selenization. These leave large pores after they are removed through KCN etching, thus causing the formation of shunt path. This means that using a Cu-rich precursor can lead to an inability to achieve acceptable value as a device. Therefore, it is recommended that DIGS thin films be fabricated from suitably Cu-poor precursors.

Acknowledgment

This research was supported by the Yeungnam University research grants in 2010.

References

- [1] T.L. Cottrell, Butterworths, *J Pediatr*, **45**, 206–209, (1954).
- [2] D.S. Albin, J.R. Tuttle, G.D. Mooney, J.J. Carapella, A. Duda, A. Mason, R. Noufi, *Proc., IEEE*, **1**, 562–569, (1990).
- [3] T. Yamamoto, M. Nakamura, J. Ishizuki, T. Deguchi, S. Ando, H. Nakanishi, S. Chichibu, *Journal of Physics and Chemistry of Solids*, **64**, 1855–1858, (2003).

- [4] M. Sugiyama, A. Kinoshita, M. Fukaya, H. Nakanishi, S.F. Chichibu, *Thin Solid Films*, **515**, 5867–5870, (2007).
- [5] O. Volobujeva, M. Altosaar, J. Raudoja, E. Mellikov, M. Grossberg, L. Kaupmees, P. Barvinski, *Solar Energy Materials & SolarCells*, **93**, 11–14, (2009).
- [6] Cherng-Yuh Su, Wei-Hao Ho, Hsuan-Ching Lin, Cuo-Yo Nieh, Shih-Chang Liang, *Solar Energy Materials & SolarCells*, **95**, 261–263, (2011)
- [7] Chandrakant D Lokhande, Gary Hodes, *Solar Energy Materials & SolarCells*, **21**, 215–224, (1987)
- [8] C. Xue, D. Papadimitriou, Y. S. Raptis, *Journal of Applied Physics*, **96**, 61–68, (2004)